Does the Concentration Principle Hold for Photographic Latent Image Formation?

Vitali V. Gavrik
Cologne, Germany

Annotation

The concentration principle appears to be an artifact of experimental techniques not a feature of photolytic process. It was usually examined after a pre-development at predominantly granular kinetics. The negatively charged developing species used in the presence of bromide antifoggant restrict silver reduction in a grain by only its largest latent image center (LIC). Bromide anions adsorb on the LICs at early development stages. Slowly penetrating developer anions gradually displace them later and the centers become developable after their bromide-free surfaces have got the critical size. The induction of large LICs is small enough for a grain to be completely developed with no influence of smaller centers.

If studied without development, the LICs coagulate during silver halide dissolution to prepare the electron microscopic samples. Evidence is considered for reshaping, mobility, and remote interactions of silver particles deprived of contact to ionic salt surface. Actual recollection of photolytic silver into a single center per grain would increase by about an order of magnitude the photographic emulsion speed.

Introduction

The concentration principle (CP) of latent image (LI) formation claims the photolytic silver to collect mostly in a single center on an emulsion grain. Together with 9 orders of magnitude LI amplification by the photographic development, it was thought to provide silver halide emulsions for the highest speed among the competing imaging systems.

The CP was usually tested with energetic negatively charged developing species of methol, hydroquinone, or ascorbate in the presence of soluble bromide to prevent from fogging. Although the developing specks number in a grain was small, it depended on the developer composition in just the first studies with the arrested development techniques,[1] representing only a part of LICs. The total LICs number in an emulsion microcrystal (MC) was recently shown to grow proportionally to the light exposure while the mean LIC size saturated soon.[2,3] The small number of developing specks per grain is shown below to be a feature of granular (GD) and early mixed development not of the LI itself.[3]

If studied undeveloped, the LI particles can readily coagulate after deprived of fixing between a MC surface and gelatin. The coagulation, induced by preparation of gelatinate shells remained from MCs after dissolving silver halide and gelatin to avoid extra silver formation and inefficient radiation absorption in electron microscopy, can drastically decrease the number of silver particles. The restricted resolution can make observable only the largest of coagulated particles.

Only the Largest Latent Image Centers in Grain Are Active by Granular and Mixed Development

The parallel development[4-6] that can simultaneously reveal all the LICs in a MC,[7,8] *has never been used in the arrested development techniques* for its fast fogging action. In the process, typical to uncharged or strongly adsorbed developing species or to negatively charged developers in absence of soluble bromide, silver mass grows with a constant rate on all the LICs until the MCs are completely reduced or a critical inhibitor concentration released:[7,8]

$$M(t) = N_E\, m_\infty\, q(t) = N_E\, m_\infty\, m_{o,E}\ k_d\,(t\text{-}t_s)\ \text{at}\ t_s < t < t_w \qquad (1)$$

where N_E and $m_{o,E}$ are the number of developable MCs and the active LI surface per MC at a given exposure, E; m_∞ is the silver mass in completely developed grain; $q(t)$ is the developed portion of MC by the time, t; k_d is the specific rate constant per active LI unit area; t_s is the initial soaking time, and t_w is the time for a MC to develop completely. The linearity conforms with the constant growth rates of silver filaments of different origin[8] and keeps until most of polydisperse MCs get completely developed.

The negative developing agents were used with bromide antifoggant, changing from the parallel to granular or mixed kinetics.[3,9] The GD slowly accumulates silver grains each of them has almost instantly developed after its induction period depending on light exposure.[10-12]

The GD rate little varies within a wide time range. On Fig. 1a, over 70% completely developed MCs accumulated linearly.[5] The curve slightly shifted to left owing to extra silver reduction without a stop-bath. A 0.67 mkm edge cubic silver bromide MC developed completely for 20 s. The covering power kept constant as it is common to the GD. Fig. 1b shows also the optical density to vary linearly with the development time in HD-2 developer (2 g KBr added to the parallel HD developer[8] that contains 6 g hydroquinone, 50 g Na_2SO_3, 50 g Na_2CO_3 per 1l solution).

Bromide penetrates gelatin an order of magnitude faster than organic molecules do.[13] Adsorbed on the LI, its anions repulse negatively charged developing species coming. While the bromide is being replaced, more and more MCs develop and *D-logE* curve, initially shifted to high exposures, shifts to its position without bromide. The gradient curves on Fig. 2 shift within over 1.0 log-exposure range.
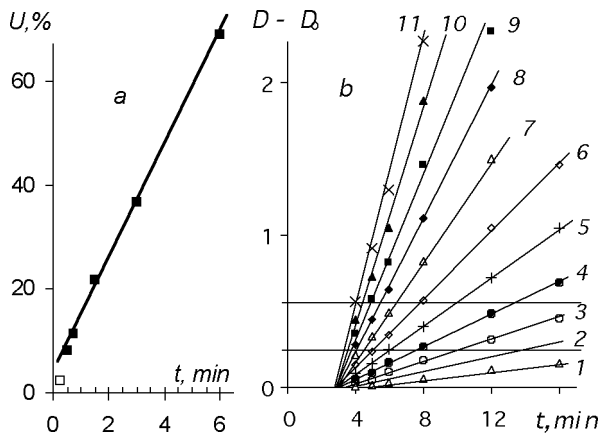
Figure 1. (a) Variation in the portion of developed microcrystals with the development time in D-72 solution. Adapted from Ref. 5. (b) Optical density dependencies on the GD time of silver iodobromide emulsion (2.3% mol. AgI). The curve numbers are successive 0.15 log-exposure steps of sensitometer wedge.
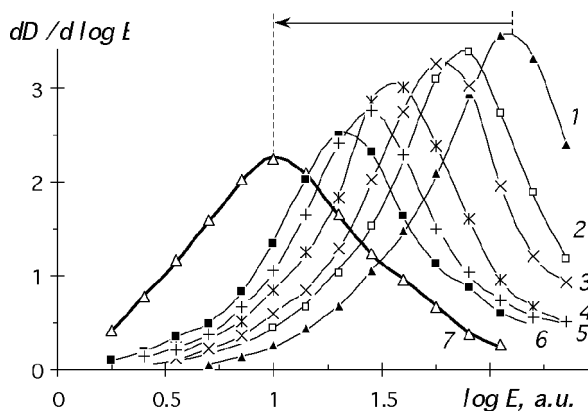

Figure 2. The gradient curves at the development times in HD-5 developer (HD, 5 g/l KBr added): (1) 16, (2) 18, (3) 20, (4) 24, (5) 28, and (6) 32 min; (7) 0.4 g/l phenidone added, 7 min.[9]

The initial shifts corresponded[3,9] to the adsorption series where an agent replaces foregoing ones from silver: CO_3^{2-}< OH^- ≈ Cl^- ≤ SO_3^{2-} << hydroquinone ≤ Br < methol < phenidon < N,N-substituted *p*-aminoaniline< CNS^- < I^- ≈ quinone.[8] They grew with bromide content and negative charge of developer: aminoaniline<methol<hydroquinone. Methol an phenidone (Fig. 3, curves 3, 4) started to replace bromide just after soaking. Hydroquinone (curves 1,2) did after its strongly adsorbing oxidation product, quinone, had accumulated on the LI. Pretreatment with diluted HD eliminated[8,9] the initial shift as the LI had been occupied by quinone that reduced by sulfite to developing species. Strongly adsorbed developers with two amino groups showed no shift of *D-logE* curves.[9]

An equilibrium portion, s_a/s, of adsorbent surface, occupied by adsorbate, is known from the physical chemistry to be constant at an adsorbent concentration. The crystal lattice of silver salts forces the LI clusters to be flat and have special orientations.[14] The LI on non-bromide salts is destroyed by light of shorter wavelength[15] and stronger oxidizer than that on silver bromide[16,17] having the lattice size correspondences to silver.[4] The spectral absorption of photolytic silver[18,19] and the *D-logE* curve constitution[2,9,20] vary in leap-like manner while the salt was gradually converted or dissolved and silver clusters acquired a three-dimensional shape.
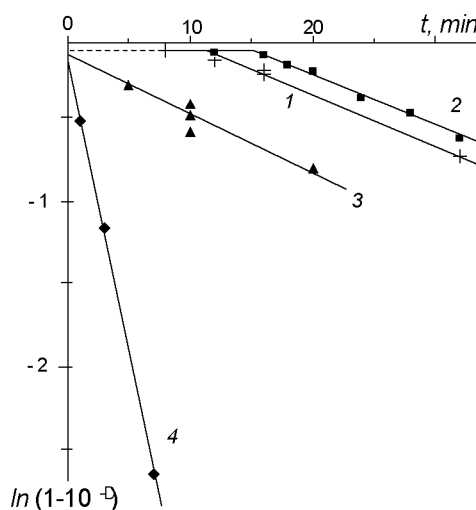

Figure 3. The shifts of D-logE curve with the development time: (1) HD-2 (developer charge and adsorption: -2, weak); (2) HD-5 (-2; weak); (3) HD-5, 1 g/l methol added (-1, moderate); (4) HD-5, 0.4 g/l phenidone added (-1, strong).
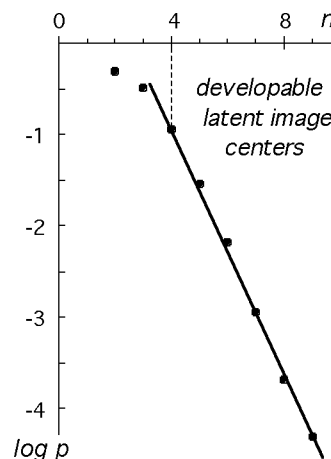

Figure 4. The size distribution density of latent image centres.[2,3,21]

The active surface of atom-thick LIC containing hardly over ten atoms (Fig. 4)[2,9] is proportional to and can be expressed as the number, *n*, of its silver atoms. Bromide adsorp-

tion proportionally decreases the catalytic surfaces of all the LICs, resulting in the shift, Δ, of *D-logE* curve along the *logE* axis:[9]

$$s_d/s = n_a/n = 10^{-\Delta} = \text{const,} \qquad (2)$$

n and n_a are the total and bromide-free active surfaces of LIC, respectively. While bromide is being gradually replaced by a developing agent, the shift decreases.

The replacement rate is proportional to the bromide-filled LI surface, $dn_a/dt = - k_r (n - n_a)$, where k_r is the rate constant. If n_k is the minimum bromide-free surface to make a grain developable, θ_{sb} is the LI surface portion occupied by bromide after swell, and t is the time of critical replacement:

$$ln(1 - 10^{-\Delta}) = ln(1- n_k/n) = ln\theta_{sb} - k_r (t - t_s). \qquad (3)$$

The fraction of grains, $U(t)$, developed by the time, t, is unity by parallel kinetics but varies from 0 to 1 by GD:

$$M(t) = N_E U(t) m_\infty q(t) = M_{\infty,E}U(t), \qquad (4)$$

$M_{\infty,E}$ is the maximum silver mass developable at an exposure. By definition, the developed portion of grain, $q(t)$, turns almost instantly into 1 after the grain has started to develop.

The process rate is controlled by the spread in MC induction times, which are in turn determined by the largest LICs in the MCs. The size distribution of LICs, analytically derived from probabilistic considerations[21] and Monte-Carlo simulated,[2,3] explained the regularly spaced development rate steps[20,22] shaping the *D-logE* curve.[23,24] Without subcritical centers ($n \leq 3$) experimentally proved[25] not to catalyze the development, the distribution becomes exponential:

$$dp(n) = K \, exp \, [-K \, (n - n_k)]dn, \qquad (5)$$

n_k is the minimum size of LIC being capable of inducing development, K is the line slope module on Fig. 4. The cumulative fraction of developable LICs, counted from the largest size, is $Q(n) = 1 - P(n) = exp \, [-K(n - n_k)]$. Then the largest LIC in the last developed grain is:

$$n = n_k - K^{-1} \, lnQ(n). \qquad (6)$$

Although the light exposure does not influence the LI size distribution (5),[2,21] the number of LICs grows proportionally and large silver clusters become more probable to arise in a MC. Since their probabilities strongly fall with size (Fig. 4), the largest center in a MC is expected to occur single. Then the fraction of centers, $Q(t)$, developable by the time, t, is close to the fraction, $U(t)$, of developed grains. From Eq. 3, the LIC size active at the time, t, is:

$$n = n_k/\{1 - \theta_{sb} \, exp[- k_r (t - t_s)]\} \qquad (7)$$

and Eqs 5, 6, and 7 give the general relation of GD:

$$M/M_{\infty,E} = exp\{-Kn_k\theta_{sb}/(exp[k_r(t - t_s)]- \theta_{sb})\}. \qquad (8)$$

Calculated at $Kn_k= 6.2$, taken from Fig. 4, as well as with assuming realistic $\theta_{sb}\cong1.0$ and arbitrary $k_r = 1$, which propor-

tionally changes the time scale, the current fraction of developed grains and so the relative silver mass have grown actually in a closely linear manner (curve 1 on Fig.5 within a wide range of development time:

$$M = D/C \cong k \, (t - t_o) \qquad at \, t > t_o, \qquad (9)$$

where $t_o = k_r^{-1} \, ln\theta_{sb}(1+ n_kK/lnU_o)+t_s$ is the induction of emulsion layer until a just perceptible fraction, U_o, of grains with large LICs has been developed. For the covering power of completely deveoped grains does not vary,[5] the optical density also grows linearly by GD (Fig. 1b).
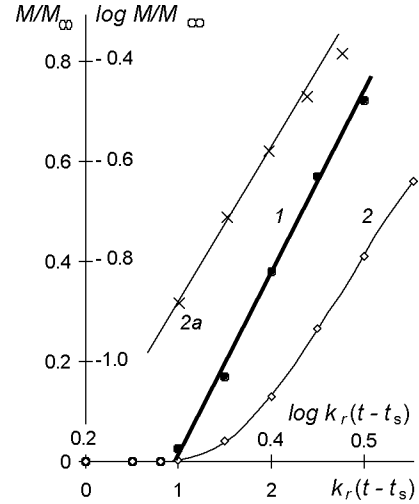

Figure 5. Simulated silver mass dependencies on the development time: (1) granular kinetics, Eq.8; (2) mixed kinetics, Eq.11; (2a) the mixed kinetics on double logarithmic scales.

Fyson and Levenson[26] observed the toe tendency of mixed kinetics to have a slope ~3 on *logD, log t* scales. They assumed autocatalysis to explain the slope as if the surface, S_{Ag}, of developing particle would have been related to its mass, M, like by three-dimensional particle growth, $S_{Ag} \sim M^{2/3}$. The time-cubed toe observed is actually inconsistent with the hypothesis. Even a just visible darkening is known to consist of filaments lengthening by orders of magnitude with constant thickness of 10 to 20 nm typically.[4,27] For filament surface grows proportionally to its mass, the actual autocatalytic rate equation, $dM/dt = k_aS_{Ag} = k'_a M$, cannot result in a cubic but in an exponential dependence on the development time, $lnM = lnM_o + k'_at$.

The time-cubed toe is produced by three almost linear dependencies multiplied at the initial stages (not over 30% silver in Ref. 26) of mixed development:

$$M \cong N_E m_\infty U(t) m'_{o,E}(t) k_d \, (t - t_s) \, at \, t > t_o, \qquad (10)$$

$m'_{o,E}(t)$ is the growing with development time, bromide-free active surface of the largest LI center in grain:

$$M \cong N_E m_\infty U(t) \, m_{o,E} \{1 - \theta_{sb} exp[- k_r(t - t_s)]\} k_d(t - t_s). \quad (11)$$

Calculated at $k_d = 0.2 \, k_r$, the silver mass growth curve 2 on Fig.5 has shown a common curvature. The toe broadened with decreasing k_r when the bromide content or developer charge increases or developer adsorption is weaker. The initial slope of kinetic dependency of mixed development is actually close to 3 on double logarithmic scales (curve 2a).

After substituting Equation 11, the time-cubed character of the toe becomes more obvious:

$$M \sim k'(t - t_o)(t - t_s)^2. \quad (12)$$

It might be the random coincidence that caused Fyson and Levenson[26] to miss the deciding relation, $S_{Ag} \sim M$, of common filamentary development that cannot result in such a time-cubed toe if the autocatalytic hypothesis is assumed.

At early stages of mixed development with low-adsorbing ascorbate, the average mass (volume) of silver particle also slightly deviates from linear growth[28,29] (Fig. 6a). The number of developing grains has no effect on the mean, and bromide replacement is slow enough for a grain to be mainly reduced with the bromide-free active surface close to the critical size. In usual methol- or phenidone-containing developers, the bromide-free LIC surface grow fast and the mixed kinetic dependency acquires the common curvature. Thus, the GD occurs in principle on only the largest LIC in a MC. Its is frequently disposed at a dislocation which retains the smallest photolytic silver species for a longer time to grow. The initial stage of typical mixed development appears also to be limited in a similar way, producing few growing silver specks per grain (Fig. 6b). *The developers used in the arrested development techniques cannot give reliable evidence for the concentration principle of LI formation.*
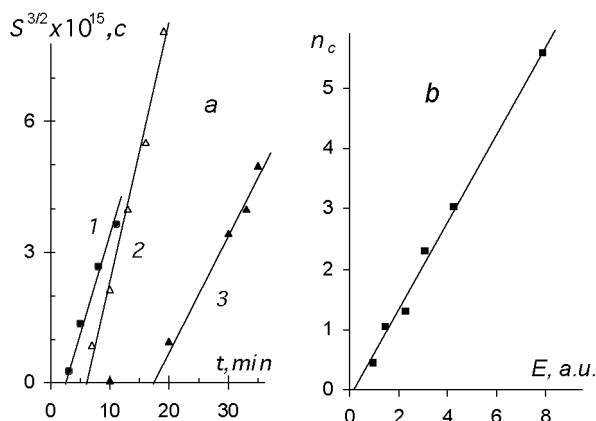

Figure 6. (a) Growth of the average volume of pre-filamentary silver specks with the time of ascorbate development. KBr: (1) 0.001, (2) 0.01, and (3) 1.0 g/l. Adapted from Pontius, et al.[28,29] (b) Dependence of silver specks number per grain at mixed development on light exposure. Adapted from Kuge.[30]

LICs Coagulation by Silver Halide Dissolution

The common preparation techniques of electron microscopic samples deprives silver from its contact with silver halide crystal lattice.[31,32] That can cause significant reshaping, mobility and coagulation of its particles at least within the after-MC voids in gelatin layer, especially in the case of non-developed photolytic silver. Studies on metals vapors showed unusual increase (at least by factor of 10^4) in the dispersion component of van-der-Waals attraction for silver particles[33,34] that was accompanied by drastic acceleration of their coagulation.[35] Silver evaporated onto a polymer and covered by gelatin readily coagulates by even soft thiosulfate solution treatment, especially if the initial particles are smaller than 5 nm.[36] The so called drop effect indicates even the developed silver to move considerably far and fast through swollen gelatin and coagulate again by slow drying of emulsion layer.[37] The empties arisen within the gelatin layer instead of MCs, whose gelatinate shells were observable after gelatin dissolution,[31,32,38] should additionally favor the ultradisperse colloid silver particles to move. The gelatin dissolution was used to prevent from inefficient electron absorption favors the reshaping and coagulation of silver particles.

It seems to be common knowledge that the number of quanta hit a MC obeys the Poisson law. In fact, the Poisson distribution plays the same fundamental role in random processes as the Gaussian one in summarizing of random variables of different origin. A composition of random processes tends also to a Poisson process. Let us consider a monodisperse photographic emulsion. Since random processes producing photolytic silver are similar in all MCs, the probability of a silver mass to arise within a MC will obey the Poisson law. Therefore, if all the silver atoms randomly produced by light in a MC actually collect themselves in a single center, the variation coefficient of LIC volume distribution should tend to that of Poisson distribution:

$$\eta_v = 1/\sqrt{v_m / v_o}, \quad (13)$$

v_m is the mean particle volume, and v_o is the volume occupied by an atom in silver crystal lattice (~0.068 nm^3). Large emulsion grains may consist of several random blocks depending on the crystal dislocations and separately collecting the photolytic silver. Relation (13) should remain true even if a MC consists of several relatively independent blocks.

Unique high-resolution data on the size distribution of photolytic silver particles were recently reported by Tani et al.[32] Monodisperse emulsion studied was 'composed of octahedral and cubic AgBr grains with average equivalent circular diameter of 0.2 mkm' that seemed sufficiently small to consist of only one block. The particle diameter, l, was measured as usually instead of particle volume. Its distribution density function, $p(l)$ relates to that of particle volume, $v = \pi \, l^3/6$, as follows:

$$p(v) = p(l)dl/dv = p(l)dl/d(\pi l^3/3) = 2p(l)/\pi l^2. \quad (14)$$

Curve 1 on Fig. 7 is particle volume histogram adapted from the large-scale graph on Fig.2 of Ref.32a with adjusting most closely to even Δv. It is monotonic, except for the initial size range close to the resolution threshold. Electron microscopic techniques used allowed to observe particles over 2 nm in size. The calculated mean particle volume, v_m^*, is 299 nm³ or about 4400 atoms, and η_v should be ~0.015 (the smallest and largest particles should hardly deviate by more than 20 nm³ from the mean). Its calculated value, $\eta_v^* = 0.63$, is over an order of magnitude larger, indicating the distribution not to obey the Poisson law (curve 2) and *the formation of photolytic silver not to follow the concentration principle.*
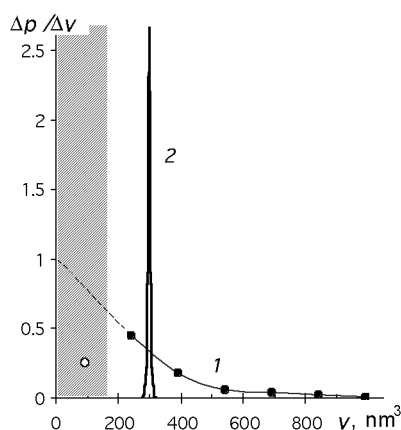

Figure 7. Distribution density functions of particle volumes: (1) experimental, adapted from Tani;³² (2) Poisson distribution (ordinates multiplied by 0.1) corresponding to the concentration principle. Shaded are sizes less or close to the resolution limit.

The mean size of photolytic silver particles was recently shown[2,3,21] to be about 3 atoms within the wide exposure range. The constant variation coefficient of the LIC size distribution, close to 0.3, kept for silver particles by the GD in the presence of potassium thiocyanate *within several orders of magnitude exposure range.*[39] The value could keep if only LIC size distribution actually obeyed Eq. (5).

The largest LICs whose size hardly exceeded 1 nm (Fig. 4) could not be observed by Tani.[32] The silver particles observed within the gelatinate shells were much larger that the LICs and might be formed by their coagulation when silver halide and bulk gelatin were dissolved to improve the resolution. The LICs number grows proportionally with the light exposure[2,21] and the numerous LICs arisen in a grain by a sufficient exposure can contain enough silver to coagulate with producing the particles of observable size.

Since coagulation is usually incomplete (complete silver collection into a single center should result in the Poisson distribution) owing to understandable mobility limitations, the Smoluchowski distribution[40] should arise. It is practically independent[21] of the initial, before-coagulation particle size distribution and coincides with the exponential distribution,

$$dp(v) = v_m^{-1} \exp[-v/v_m]dv, \qquad (15)$$

which is notable for its strongly predominating probabilities of small particles to coexist with solitary large particles like those observed. Its variation coefficient, $\eta_v \to 1.0$, if all the ultimate particles were taken into account.[21]
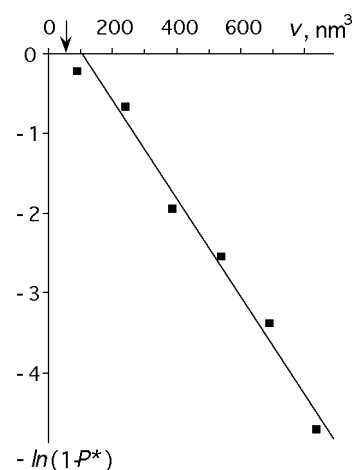

Figure 8. Experimental size distribution of photolytic silver particles within the gelatinate shells after AgBr and gelatin dissolution. The arrow indicates the resolution claimed. Adopted from Tani.³²

The exposure considered corresponded to the beginning of the plateau of *D-logE* curve[32] and seemed to provide for a silver mass enough to make the largest coagulated particles quite observable. The volume distribution density function of particles exceeding the resolution threshold, v_r, will be:

$$dp^*(v) = v_m^{-1} \exp[-v_r/v_m]\exp[-v/v_m]dv \qquad (16)$$

and their volume distribution function,

$$P^*(v) = 1 - \exp[(v_r - v)/v_m]. \qquad (17)$$

Then the $ln(1-P^*)$ dependence on the particle volume should be linear with the slope, $-1/v_m$, and $v = v_r$ at $ln(1-P^*) = 0$.

The calculated mean of the experimental distribution is $v_m^* = v_m + v_r$, and its variation coefficient:

$$\eta_v^* = v_m/(v_m + v_r). \qquad (18)$$

Fig. 8 demonstrates the dependence to be actually linear. It gives $v_m^* = 264$ nm³ and $\eta_v^* = 0.62$ practically coinciding with the results of direct statistical calculations above. Thus, *the main process responsible for the formation of silver particles observed within the gelatinate shells should be the coagulation of initial LICs during the sample preparation for electron microscopy.* The small-scaled histogram on Fig. 1 of Ref. 32 was of the same type and its size spread was no smaller than that considered. It characterized similar emulsion without reduction sensitization at much higher exposures corresponding to the shoulder of its *D-log-E* curve.
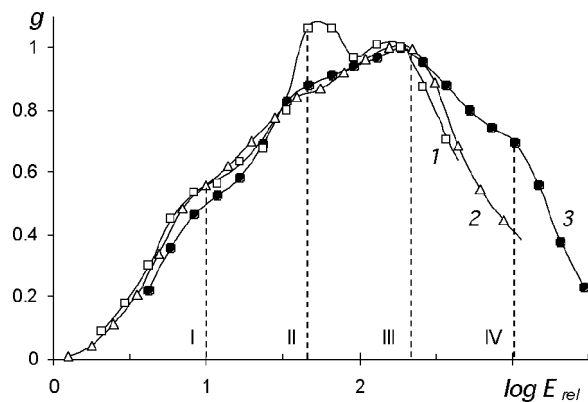
Figure 9. The gradient curves by parallel development: (1) 0.1, (2) 0.1, and (3) 0.6 mkm^2 mean MC projective area. Roman numerals denote the successive development rate steps caused by one-atom increments to the LI centers in the MCs.

The mobility appears to be restricted for silver produced with reducing agents and more strongly attached to gelatinate shells. If chemically reduced, silver arises in the same site where the reducer transforms into an oxidizer favoring extra metal-polymer binding with gelatin.[41] Oxidized developing agents are known to produce the denaturated gelatin shells on developed silver filaments.[42] This restricts mobility of chemically reduced silver particles, preventing them from coagulation as well as from any kind of participation in LI formation except for the deactivation of photolytic halogen.[4]

The reduction sensitization silver particles remained numerous (up to 600 centers on each grain[31]) after growing to the observable sizes. The developed particles in the tests by Klein[39] kept the log-volume standard deviation, $\sigma[lnv] \cong \eta_v \cong$ 0.3, of LI size distribution (5) undistorted by the preparation procedures for electron microscopy. The light exposure releases halogen oxidizer far from silver particles produced. LIC binding to gelatin is weaker and favors coagulation of photolytic silver in the dissolving MC.

The small silver halide MCs and long low-intensity exposures used in Ref.32 have no advantages in demonstrating the CP. The regular multi-stepped structure of *D-logE* curves also induced[2,3] by the LIC size distribution (5) has hold for even 0.1 mkm MCs (curve 1 of Fig. 9). The structure did not disappear at long exposures (at least up to 1h) to low-intensity light. The data by Klein[39] also showed no transition of variation coefficient to the small values of Poisson distribution that would have followed from the CP.

Actual Single-Particle Silver Recollection

What is the increase in emulsion speed expected by actual single-particle silver recollection? What way may it be performed in commercial layers? The paper volume does not allow us to consider in details the matters.

The threshold sensitivity can increase at the expence of subcritical particles of photolytic silver, that are unable to catalyze the photographic development. Their light absorption, measured by Nail et al.[43] in a transparent ultradisperse emul-

sion layer, was several times larger than that corresponding to the developed density threshold, indicating them to be much more numerous than the LICs of critical size.

If the threshold sensitivity is provided by MCs containing a 4-atomic LIC, the number of 3-atomic centers should be in average about three times larger, and that of 2-atomic centers about five times larger (Fig. 4). The total silver content of such a MC is then about 25 silver atoms. If all the photolytic silver was collected in a single LIC, the light exposures producing 4-atomic particles in the same fraction of MCs could be 6 times lower. This corresponds to 6-fold increase in speed, or 2.5 stops more than that of common emulsion of the same grain size. The contrast should also increase as the LIC size growth would obey the Poisson law whereas the resolution and granularity could obviously remain at the same level as earlier.

Conclusion

There is no reliable evidence for the concentration principle to hold for the latent image formation in the silver halide photography. Bromideless parallel developers that reveal all the latent image centers in a grain have never used in the arrested development techniques because of fast fogging. The granular or mixed developers used occur in principle on one or a few larger latent image centers in grain.

The sample preparation for electron microscopy removes silver halide and gelatin, thus inducing fast coagulation of initial photolytic silver and causing the Smoluchowski size distribution with rare large particles over the resolution threshold. Its particle variation coefficient is two orders of magnitude larger than that of Poisson distribution that would result from the concentration principle. Resolution restrictions make observable only the largest coagulated particles. Silver reduced by chemicals is often more strongly fixed to the gelatin shell of MC by extra metal-polymer bonds induced by oxidizer released.

Acknowledgement

References

1. Spencer, H. E., and Atwell, R. E., *J. Opt. Soc. Am.*, **54**, 498 (1964); **56**, 1095 (1966).
2. Gavrik, V. V., *IS&T's 48th Ann. Conf.*, Washington, 246 (1995); *Sci. Appl. Phot. Cinem.* **41**, 58 (1996).
3. Gavrik, V. V*., Int. Congr. Imag. Sci., Antwerp* **1,** 419 (1998); *Imag. Sci. J. (J.Phot.Sci.),* **47** (1999), in print.
4. Mees, C. E. K. and James, T. H., *The Theory of the Photographic Process*. 3-rd edn (1966).
5. Miyake, K. and Tani, T., *J. Imag. Sci. Technol.* **39**, 355 (1995).
6. Farnell, G. C. and Jenkins, R. L., *J. Photogr. Sci.* **29**, 39 (1981).
7. Gavrik, V. V., *IS&T's 50th Ann.Conf., Cambr., Mass.* 57 (1997).
8. Gavrik, V. V., *Imag. Sci. J.* (*J. Phot. Sci.*) **46**, 32, 45 (1998).
9. Gavrik, V. V., Barantseva, G. I., and Kononova, O. N., *J. Inf. Rec. Mater.* **13**, 409 (1985).

10. Sheppard, S. E. and Mees, C. E. K., *Investigations on the Theory of the* Photographic *Process*, 1907.

11. Sheppard, S. E., *Photogr. J.* **59**, 135 (1919)

12. Trivelli, A. P. H., *J. Franklin Inst.* **241**, 1 (1946).

13. Iwano, H., *J. Photogr. Sci.* **20**, 135 (1972).

14. Berry, C. R. and Griffith, R. L., *Acta Cryst.* **3,** 219, 247 (1950); **6**, 94 (1953).

15. Bartelt, O. and Klug, H., *Z. Physik* **89,** 779 **(**1934).

16. Sutherns, E. A., *J. Photogr. Sci.* **8,** 118 (1960);

17. Hautot, A., *Sci. Ind. Photogr.,* Ser.2, **23,** 409 (1961).

18. Gavrik, V. V. and Barantseva, G. I., *IS&T's 49th Ann. Conf.*, Minneapolis, 59 (1996).

19. Gavrik, V. V. and Barantseva, G. I., *Optics & Spectr.* **83**, 701 (1997).

20. Gavrik, V. V. et al., *J. Inf. Rec. Mater.* **8**, 83,167 (1980).

21. Gavrik, V.V., *Silver Halide Imaging Symp., Victoria,* 37 (1997).

22. Gavrik, V. V., *J. Inf. Record. Mater.* **3**, 125, 133 (1975).

23. Silberstein, L. & Trivelli, A.P.H., *J. Opt. Soc. Am.* **35**, 93 (1945).

24. Pitt, D. A., Rachu, M. L., and Sahyun, M. R. V*., Phot. Sci. Eng.* **21**, 331 (1977).

25. Fayet, P., Granzer, F., Hegenbart, G., et al., *Z.Phys.* **D3**, 299 (1986)

26. Fyson, J. R. and Levenson, G.I.P., *J. Photogr. Sci.* **25**, 147 (1977).

27. Farnell, G. C. and Solman, L.R. *J. Photogr. Sci.*, **18**, 94 (1970).

28. Pontius, R. B. and Willis, R. G., *Phot. Sci. Eng.* **17**, 21, 157 (1973).

29. Pontius, R. B., Willis, R. G., and Newmiller, R. J., *Phot. Sci. Eng.* **16**, 406 (1972).

30. Kuge, K., *J. Soc. Phot. Sci. Techn. Japan,* **42**, 320 (1979).

31. Hammer, F. A., Comer, J. J., *J. Appl. Phys.,* **24**, 1495 (1953).

32. a) Tani, T., Tasaka, T., and Murofushi, M., *Int. Congr. Imag. Sci., Antwerp*, **1,** 239 (1998); b) *PICS'99 Conf., Savannah (this book).*

33. Stockham, J. and Homer, J. B., *Disc. Faraday Symp.*, **7**, 85 (1973).

34. Burtscher, H. and Schmidt-Ott, A., *Phys. Rev. Lett.* **48**, 1734 (1982).

35. Okuyama, K., Kousaka, Y., and Hayashi, K., *J. Coll. Interf. Sci.*, **101**, 98 (1984).

36. Galashin, E. A., Senchenkov, E. P., Fedorov, Yu. V., and Chernov, S. F., *Sci. Appl. Phot. Cinem.* **28**, 67 (1983).

37. Mees, C.E.K., *The Theory of the Photographic Process* (1942).

38. Farnell, G. C., Flint, R. B., and Chanter, J. B., *J. Photogr. Sci.*, **13**, 25 (1965).

39. Klein, E., *Mitt. Forshungslab. AGFA-Gevaert* **2**, 80 (1958).

40. Smoluchowski, M., *Kolloid Z.* **21**, 98 (1917).

41. Andrews, M.P. and Ozin, G.A., *Chemistry of Materials,* **1**, 174 (1989).

42. Lin Yuan-Sheng and Jen Hsin-Min, *J. Photogr. Sci.* **31**, 192 (1983).

43. Nail, N. R., Moser, F., and Urbach, F., *J. Opt. Soc. Am.,* **46**, 218 (1956).